Stress state of embedded Si nanocrystals

K. Kleovoulou and P. C. Kelires*

Research Unit for Nanostructured Materials Systems, Department of Mechanical and Materials Science Engineering, Cyprus University of Technology, P.O. Box 50329, 3603 Limassol, Cyprus

(Received 27 March 2013; revised manuscript received 18 July 2013; published 21 August 2013)

Monte Carlo simulations shed light on the stress state of Si nanocrystals embedded in amorphous silica, unraveling and explaining its nature and origins. This is achieved by generating detailed stress maps and by calculating the stress profile as a function of size and distance between the nanocrystals. For normal oxide matrix densities, the average stress in the nanocrystal core is found to be compressive, reaching values of 3–4 GPa, in excellent agreement with experimental measurements. It drastically declines at the interface, despite the existence of several highly strained geometries. Tensile conditions prevail in nanocrystals embedded in densified silica matrices. The nanocomposites are shown to be stable, at close interdot distances, against segregation and phase separation.

DOI: 10.1103/PhysRevB.88.085424 PACS number(s): 61.46.Hk, 62.23.Pq, 62.25.−g, 68.35.Ct

I. INTRODUCTION

Stress is well known to have profound effects on the optoelectronic properties of semiconducting systems, by shifting the band offsets and influencing the carrier dynamics, the recombination properties, and the optical absorption.[1] Such effects are pronounced at the nanoscale, where length scales are small and structural inhomogeneities are common. A prototypical nanomaterial, where stress effects are expected to be strong, consists of silicon nanocrystals (Si-NCs) embedded in amorphous silica (a-SiO_2).[2] This system has attracted considerable attention for its light absorption and emission properties. Promising applications include light-emitting devices,[3] nonvolative memory systems,[4] and third-generation solar cells.[5,6]

Despite its apparent importance, the nature and the origins of the stress state of Si-NC/a-SiO_2 remain vague. A number of experimental works refer to NCs under compressive stress,[7–10] but NCs under tension have also been reported,[11] while theoretical studies are inconclusive.[12,13] Most importantly, stress maps which can describe the details and decompose the stress state into each of the components of the nanocomposite system, i.e., the NC core, the interfacial region, and the matrix, are lacking. This is crucial for understanding the optoelectronic response of the system and for designing optimum arrangements of embedded Si-NCs. The important role of the strain of interacting NCs on the optical properties was recently demonstrated.[14] Curvature effects on the optical properties were also studied.[15]

An important issue is whether stress is distributed uniformly throughout the NC or accumulated at the interface or in the interior. This is not clarified by the experiment. In an earlier work,[2] we showed that the NCs are heavily strained and distorted in the interfacial region, to accommodate the incompatibility with the host oxide matrix, with increasing distortions in the interior as they become smaller. This is confirmed by recent investigations.[16] However, it is still unclear if the induced strains at the interface generate locally excessive stress or, instead, alleviate stress.

Another issue regards the stress state and the stability of Si-NCs positioned at short distances. Such arrangements are necessary in order to have efficient separation and transport of optically generated carriers for solar cell applications and thus have to be checked against possible instabilities.

Here, we shed light on these issues through atomistic Monte Carlo (MC) simulations. The stress state as a function of size and distance between the NCs is reported, and its origins are unraveled and explained. Also, detailed stress maps across the nanocomposite systems are generated. This is made possible by resolving the stress fields at the atomic level. In addition, we investigate the stability of strongly interacting NCs at short distances and small sizes, and we show that stress can be tailored and even reverse sign by adjusting the matrix density of the system.

The paper is organized as follows. In the next section, the Monte Carlo simulational method used to construct and extract the properties of embedded Si-NCs is described. In Sec. III, the results and the associated discussion are given. Conclusions are given in Sec. IV.

II. METHODOLOGY

For the simulations, we use cubic computational cells consisting of spherical NCs embedded in a-SiO_2 matrices. They are obtained by continuous-space MC simulations[17] using the empirical potential approach. Although less accurate than first-principles calculations, this approach provides great statistical accuracy and can probe local properties, such as the local stress field discussed below, which are intractable by quantum calculations.

For the interactions, we use the Tersoff empirical potential[18] parametrized to describe SiO_2 systems.[19] This potential describes well the elemental Si properties, silica polymorphs, and phase transitions between them, as well as the structure and energetics of a-SiO_2. In particular, the original Tersoff Si potential was fitted to the lattice constant (5.43 Å), bulk modulus (98 GPa), and elastic constants of elemental Si and is therefore expected to accurately describe bond length variations and moduli of Si NCs. The Si-O interactions yield very good agreement with experiment and *ab initio* calculations[20] for the structural parameters, density, and cohesive energies of silica polymorphs.[19] As a further test, we calculated the bulk moduli of various polymorphs. For β-cristobalite, used here to produce the amorphous oxide matrix (see below), we find a bulk

modulus of 135 GPa compared to 120–130 GPa as predicted by *ab initio* calculations.[20] For other polymorphs, such as β-tridymidite (hex), stishovite, coesite, α-quartz, and β-quartz we find moduli of 119, 320, 88, 56, and 146 GPa, respectively, compared to 130–140, 261–324 (313), 88–93, 31–50 (34–37), and 122–135 GPa from *ab initio* calculations and experiment (in parentheses). The pressure for the phase transition between the a-quartz and coesite structures is 1.7 GPa,[19] in very good agreement with experiment (1.8–2.2 GPa). The pair correlation functions of amorphous silica, as calculated by Munetoh *et al.*[19] and confirmed by us, are in good agreement with experiment and *ab initio* calculations. These tests reassure us that the pressure exerted by the amorphous matrix on the nanocrystals is correct. The potential was also recently shown to successfully treat the planar c-Si/c-SiO_2 interface, especially regarding the sensitive thermal-contact-resistance properties.[21]

One starts with Si NCs embedded in crystalline β-cristobalite.[2] The amorphization of the embedding matrix is achieved by melting and subsequent quenching from the liquid, while keeping the positions of the atoms in the NCs fixed and running the simulations in the (N,V,T) canonical ensemble. After quenching, an annealing cycle in the (N,P,T) isobaric-isothermal ensemble follows to allow for full equilibration of the nanocomposite system, both geometrically and compositionally. This is crucial for the proper structural relaxation and the formation of optimum chemical bonding at the interface region that minimizes the free energy. Finally, the structures are brought to 300 K where all properties are obtained as ensemble averages.

We have generated in total seven different composite structures with the size of the NCs ranging from 1 to 5 nm in diameter, the number of Si atoms in the NC from 40 to 3600, and the number of atoms in the oxide from 4800 to 50 000. We keep the Si/O ratio at about 0.53 to consistently capture the variation of stress with the NC size. In order to study the interaction and stability of NCs at various interdot distances, we have also generated nine different structures containing a 3-nm NC in matrices with varying sizes. The cells are subjected to periodic boundary conditions so that the NCs properly interact with their images. This mimics ordered arrangements in experimental Si-NC superlattices.[6]

III. RESULTS AND DISCUSSION

We begin with the microstructure of the nanocomposite systems. A representative example of a fully relaxed structure is shown in Fig. 1(a). The components of the system are clearly indicated. Their identification is based on the distribution of Si suboxides, i.e., of Si atoms characterized by their oxidation state (number of oxygen neighbors), which is presented in Fig. 1(b). The core of the NC is composed of Si atoms having as neighbors only Si^{+0}, i.e., Si atoms not bonded to any O atoms. The outer shell of the NC forms the inner part of the interface. It mostly contains Si^{+1} and Si^{+2} and contains a few Si^{+0}. Si^{+3} mainly occurs in the outer part of the interface, while the oxide matrix is dominated by Si^{+4} suboxides. The width of the interface is ~0.8 nm.

We find several Si-O-Si bridge bonds at the interface, as in our previous studies[2] using a simpler (Keating) valence force

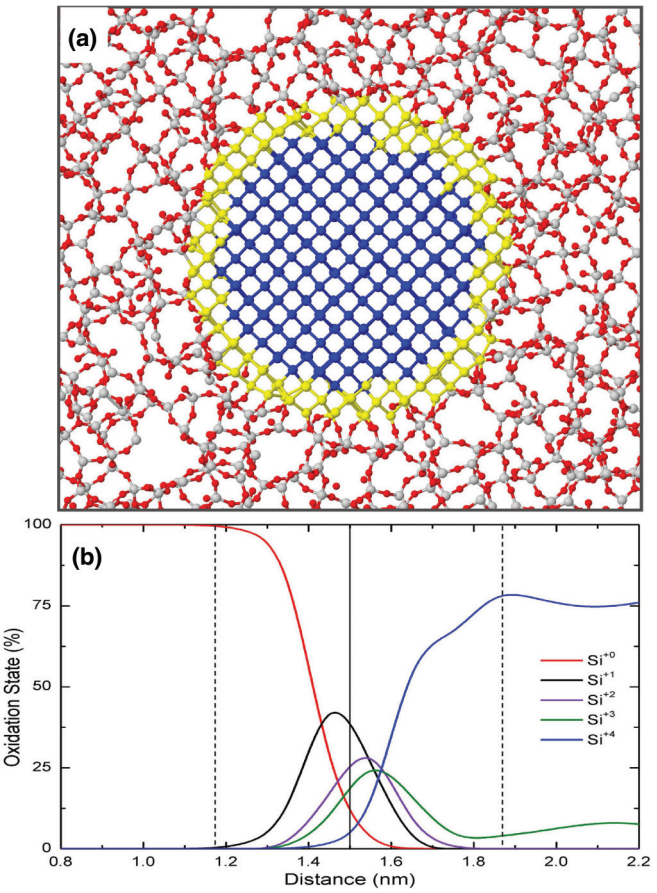

FIG. 1. (Color online) (a) Ball and stick model (thin slice cut) of a Si-NC/a-SiO_2 nanocomposite. Part of the matrix is shown. The size of the NC is 3 nm. The distance from its images is 6.2 nm. Core (outer shell) Si atoms in the NC are shown in blue (yellow). Matrix Si and O atoms are colored gray and red, respectively. (b) Distribution of suboxides as a function of the distance from the NC's center. Vertical solid (dashed) lines denote the nominal position (extent) of the interface.

model. The present model, contrary to the Keating model, does not strictly impose fourfold and twofold coordination for Si and O, respectively, and so in principle allows for more complex bonding at the interface, such as for Si=O double bonds. Still, no such bonds are found, indicating their high formation energies. There are, though, some Si coordination defects.[22,23] These findings are in accord with other simulational studies.[12] The equilibrium density of the oxide matrix in all cells is 2.2 gcm^{-3}, as is the bulk density of a-SiO_2 with the present model. Experimental values range from 2.2 (normal value)[24] to 2.6 gcm^{-3} (densified silica glass).[25]

We now proceed to the study of the stress state of Si-NC/a-SiO_2 nanocomposites. Significant insight is obtained when the stress field is analyzed locally, using as a probe the tool of atomic level hydrostatic stresses.[26–28] A contour map of atom-projected stresses in our representative structure, at its equilibrium matrix density, is shown in Fig. 2. There are two notable findings in this map. The first is that the stress field in the NC is compressive and nonuniform. The second, and most striking, is that the stress is much higher in the core of the NC

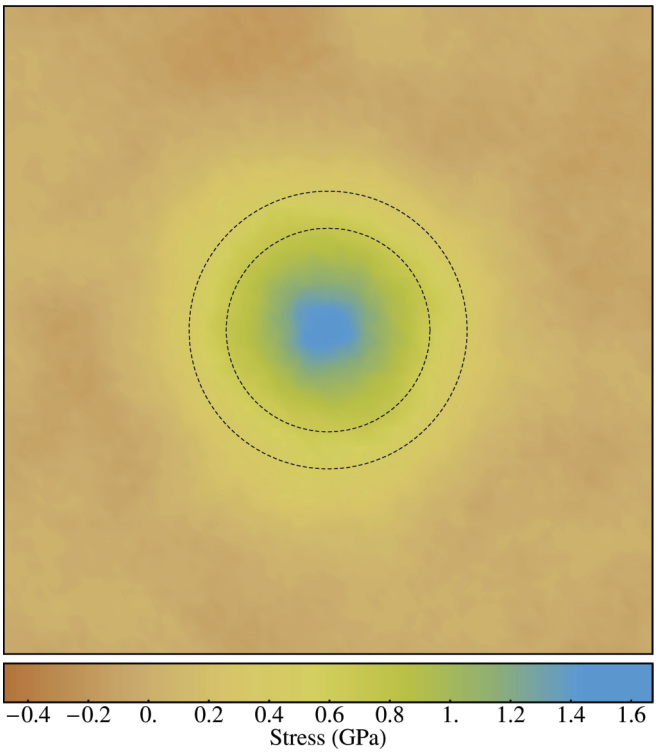

FIG. 2. (Color online) Contour stress map of the representative structure (3-nm NC). The atomic stresses are merged into a continuous mesh by averaging over spheres of 4 Å in radius. Sign convention: Positive (negative) values denote compressive (tensile) stresses. Inner and outer circles denote the boundaries of the core and the nominal interface, respectively.

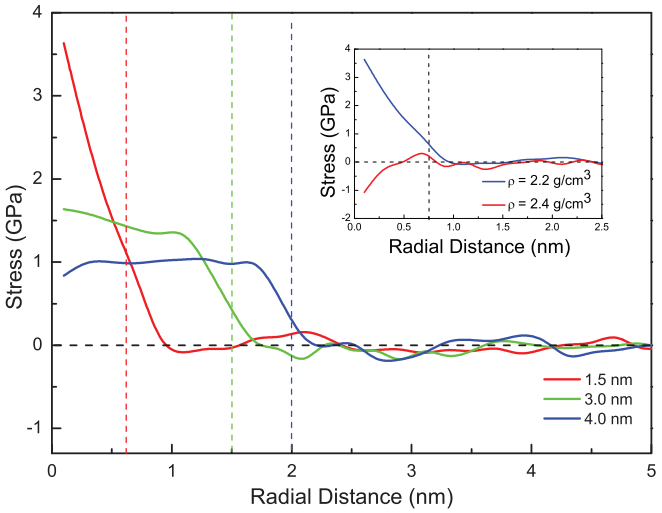

FIG. 3. (Color online) Radial variation of stress, averaged over 2-Å-wide shells, for three NC sizes. Vertical dashed lines denote the nominal interfaces. Inset: Stress variations in structures with different matrix densities.

(∼1–1.5 GPa), rather than in the outer shell at the interface. One sees that stress progressively declines moving from the center outwards and practically vanishes in the outer region of the interface. Stress in the oxide is nearly neutral, except near and around the interface where it is slightly tensile. This is the general trend in all structures studied.

Firm experimental evidence for compressive stress in Si-NC/a-SiO_2 is provided by several recent Raman measurements.[7–10] Its importance for the light-emission properties was recently demonstrated.[29] In these studies, however, no information on the stress distribution is provided. Values range from hundreds of MPa to a few GPa, depending on the NC size. Previous simulations[13] found tensile stress in the NC core, for normal oxide matrix densities, in sharp disagreement with experiment and our results. The origin of this discrepancy is not clear. Note that the possibility for tensile stress has also been reported by Raman studies,[11] but in another context. We discuss this possibility below.

The finding that stress is higher in the core than in the outer shell at the interface might be thought of as counterintuitive, considering that bond length and angle distortions are found to be much higher in the latter than in the former.[2,16] To explain this effect, let us first assume that a particle with density ρ_2 is embedded and grows in a matrix with density $\rho_1 < \rho_2$ forming an abrupt interface with zero width. The particle, being the "minority element,' tries to conform to its environment. Thus, it desires to relax its density toward ρ_1 by expanding its volume. Due to the much larger size/volume of the matrix and the rigid interface, this is not possible, and thus the particle feels uniformly compressed by the matrix. The effect will be enhanced if the thermal expansion coefficient of the particle is larger than that of the matrix, as is the case here.[7] This compressive stress is the equivalent of the hydrostatic pressure which would shrink the diameter of the particle from the "desired" to the "actual" one.

Now, consider a nonrigid, nonabrupt interface, as in the present case. A "chemical interaction" of the matrix with the particle takes place. The formation of an interface layer with mixed chemical bonds, such as the suboxide layer here, produces a penetration of the particle into the matrix and vice versa. This allows the outer shell of the particle to partially relax the compressive stress imposed by the matrix. At the same time, the intrusion of the matrix into the particle causes its core to shrink, increasing its density to values higher than the bulk value. Indeed, we find for the 3-nm NC of Fig. 2 a core density of 2.34 gcm^{-3}, compared to the 2.31 gcm^{-3} Si bulk value with the present model. In this way, a nonuniform stress profile arises. The larger the interface width (IW), compared to the size of the particle, the larger the compressive stress and density in its core is expected to be (the variation is given below).

Therefore, the larger strains seen in the outer shell of the NC do not imply larger average stress in this region, as is widely believed. Instead, their generation partially alleviates stress. These ideas are demonstrated more quantitatively by plotting the radial dependence of local stresses from the NC center outwards, as is shown in Fig. 3 for three different NCs. For the larger NC (4 nm), the matrix effect is relatively weak because the IW to NC size ratio is small. As a result, the compressive stress in the core is low and constant, exhibiting rigid-interface behavior, and declines only close to the nominal interface. As the IW to NC size ratio becomes larger, stress rises dramatically in the core with a nonrigid-interface variation. In all cases, the average stress over the entire nanocomposite is zero, since the compression in the NC is

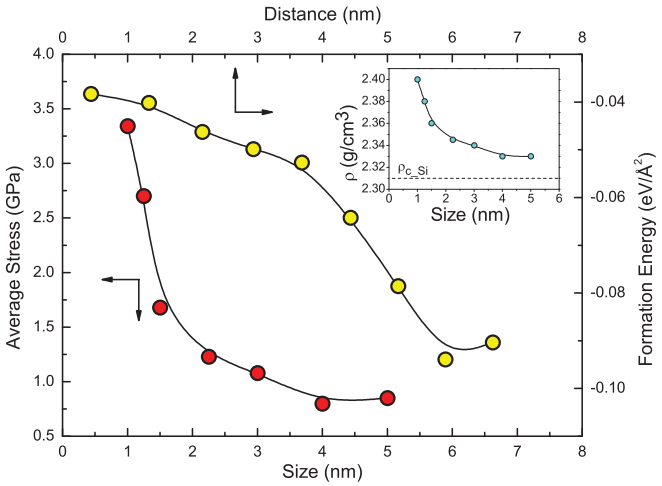

FIG. 4. (Color online) Average core stress vs NC size (red circles) and formation energy vs NC separation for 3-nm NCs (yellow circles). Inset: Variation of core density vs NC size.

compensated by the small, but over larger regions, tensile stresses in the oxide matrix.

The compression and the higher density in the core of the representative NC is also verified by the calculated average Si-Si bond lengths, which are found to be shorter by ∼1.5% compared to the bulk Si value. This is consistent with preliminary calculations of the bulk modulus of the NC, showing enhancement from the bulk value (the elastic properties and rigidity will be presented elsewhere). On the other hand, bond-angle deviations from tetrahedrality are minimal in the core. However, in the suboxide interface layer, where the average compression declines, the situation is complicated. Bond lengths are not the sole indicators of local strain because here bond-angle deviations are larger (∼2–3%); a significant part of stress relaxation occurs through them. We discuss the implications of strained geometries at the interface below.

Having elucidated the origin and nature of stress, we now examine how it varies as a function of size and distance between the NCs. Our calculations are summarized in Fig. 4. We see that the average core stress rises sharply with decreasing NC size, while keeping the NCs at large distances (⩾3 Å), reaching values of more than 3 GPa for sizes less than 2 nm. This variation is in excellent agreement with the results of Raman measurements.[7–9] The trend is also consistent with the variation of core density with NC size, shown in the inset of Fig. 4. For the smaller NC (1 nm) the increase of density with respect to the bulk value is ∼4%. Note that a finite non-negligible compression remains for even the larger NCs studied.

Figure 4 also shows the variation of the formation energies E_F of the embedded NCs. E_F is defined[2] as the total energy of the nanocomposite system relative to the sum of the cohesive energies (chemical potentials) of its constituents (NC and oxide matrix), all calculated at 300 K, normalized by the surface area of the nominal interface. The constituent cohesive energies equal the respective chemical potentials (cohesive energies per atom) of the bulk materials (crystalline Si and amorphous silica) times the number of atoms in the constituent. The results demonstrate that the E_F of strongly interacting NCs remains negative for the shortest interdot distances studied. This indicates stability against segregation and phase separation of the constituents into larger areas, especially at high-growth Ts, which would destroy the character of the nanocomposite as such. For example, in the case of 3-nm NCs at an interdot distance of just 0.4 nm, in a cubic ordered arrangement, E_F is about -40 meV/Å^2, which is quite significant in the scale of thermal energies. The stability of such NC arrangements at close distances is important for the realization of third-generation solar cells.[5,6]

All results given above refer to nanocomposites having the equilibrium oxide matrix density. However, since the experimental density of a-SiO_2 varies, due to voids, it is useful to know how stress is influenced by these density variations. To investigate this effect, we carried out a series of calculations imposing each time a different density to the matrix, from ∼2 to 2.5 gcm^{-3}. The results show that stress in the NCs not only may vary by several GPa but it might also reverse sign and become tensile. This is demonstrated in the inset of Fig. 3, where the compressive stress in a 1.5-nm NC with $\rho_0^{matr} = 2.2$ gcm^{-3} is contrasted with the tensile stress in the same NC embedded in $\rho_0^{matr} = 2.4$ gcm^{-3}.

In this case, the effect is reversed. The NC is found in a denser host environment. Thus, it desires to increase its density by reducing its volume, but the matrix tends to prevent the NC from doing so. If the interface were abrupt and rigid, that would impose a uniform tensile stress in the NC. With the formation of a flexible suboxide layer, tension progressively declines while moving from the core outwards to the mixed bond region, with slight oscillations in the near-oxide region.

Evidence for tensile, instead of compressive, stress in embedded Si-NCs is provided by Raman studies.[11] The effect was attributed to the type of the substrate and the difference between its thermal expansion coefficient and that of the Si-NC/a-SiO_2 film. This is an alternative way to tailor stress, especially at high-growth Ts. Here, instead, the effect is intrinsic. The importance of variations in the matrix density was also pointed out by *ab initio* calculations,[16] which nicely demonstrated their influence on the alignment and separation of the highest occupied molecular orbital (HOMO) and lowest unoccupied molecular orbital (LUMO) energy levels of both the NC and the matrix. The shifts of these levels is caused by the change in the stress character of the nanocomposite.

The elucidation of the stress profile of Si-NCs/a-SiO_2 may serve as a guide for unravelling the origins of optical absorption in this material. This issue has not yet been clarified, although significant progress has been made in this direction.[14–16] Understanding how stress influences the band offsets, the gap size, and intraband/interband transitions is very useful, but still does not answer the question of which are the strong absorbing centers in the nanocomposite. As Li *et al.* showed,[16] the HOMO states are mostly localized at the interface while the LUMO states are extended over the entire NC. This, along with our findings that stress is substantial in the interior and that there are strained geometries at the interface, leaves open several possibilities for the absorbing centers. Earlier suggestions for such centers include Si=O double bonds,[30,31] Si-O-Si bridge bonds,[2,32–34] and strained

bonds/geometries.[2,34,35] The former seem to be rather unstable. The latter, in view of the present results, may also be associated with inner regions of the NC. In any case, the relative contributions of these centers are unknown. Work to elucidate this important issue is in progress.

IV. CONCLUSIONS

In conclusion, our MC simulations have been able to map in detail the stress field in Si-NC/a-SiO_2 nanocomposites and to unravel its origins. For normal oxide matrix densities, the NCs are under compressive stress in the interior, which drastically declines at the interface. Tensile conditions may prevail for denser silica matrices. The nanocomposites are shown to be stable at close interdot distances.

ACKNOWLEDGMENTS

Discussions with A. Georgiades and G. Constantinides are gratefully acknowledged. This work was supported by Project ΔΙΔΑΚΤΩΡ/ΔΙΣΕΚ/0308/13 of DESMI 2008, which is cofinanced by the European Regional Development Fund, the European Social Fund, the Cohesion Fund, and the Research Promotion Foundation of the Republic of Cyprus.

*pantelis.kelires@cut.ac.cy

[1]For a recent book review, see Y. Sun, S. Thompson, and T. Nishida, *Strain Effects in Semiconductors* (Springer, New York, 2010).
[2]G. Hadjisavvas and P. C. Kelires, Phys. Rev. Lett. **93**, 226104 (2004); Phys. E **38**, 99 (2007).
[3]L. Pavesi, L. Dal Negro, C. Mazzoleni, G. Franzo, and F. Priolo, Nature (London) **408**, 440 (2000).
[4]S. Tiwari, F. Rana, H. Hana, A. Hartstein, E. Crabbe, and K. Chan, Appl. Phys. Lett. **68**, 1377 (1996).
[5]G. Conibeer, M. Green, R. Gorkish, Y. Cho, E. Cho, C. Jiang, T. Fangsuwannarak, E. Pink, H. Huang, T. Puzzer, T. Trupke, B. Richards, A. Shalav, and K. Lin, Thin Solid Films **511**, 654 (2006).
[6]P. Löper, R. Müller, D. Hiller, T. Barthel, E. Malguth, S. Janz, J. C. Goldschmidt, M. Hermle, and M. Zacharias, Phys. Rev. B **84**, 195317 (2011).
[7]T. Arguirov, T. Mchedlidze, M. Kittler, R. Rölver, B. Berghoff, M. Först, and B. Spangenberg, Appl. Phys. Lett. **89**, 053111 (2006).
[8]S. Hernandez, A. Martinez, P. Pellegrino, Y. Lebour, B. Garrido, E. Jordana, and J. Fedeli, J. Appl. Phys. **104**, 044304 (2008).
[9]I. Crowe, M. Halsall, O. Hulko, A. Knights, R. Gwilliam, M. Wojdak, and A. Kenyon, J. Appl. Phys. **109**, 083534 (2011).
[10]G. Zatryb, A. Podhorodecki, X. Hao, J. Misiewicz, Y. Shen, and M. Green, Nanotechnology **22**, 335703 (2011).
[11]Y. Tao, Y. Zuo, J. Zheng, C. Xue, B. Cheng, Q. Wang, and J. Xu, Chin. Phys. B **21**, 077402 (2012).
[12]M. Ippolito, S. Meloni, and L. Colombo, Appl. Phys. Lett. **93**, 153109 (2008).
[13]D. Yilmaz, C. Bulutay, and T. Çağin, Appl. Phys. Lett. **94**, 191914 (2009).
[14]R. Guerra and S. Ossicini, Phys. Rev. B **87**, 165441 (2013), and references therein.
[15]P. Carrier, Phys. Rev. B **80**, 075319 (2009).
[16]T. Li, F. Gygi, and G. Galli, Phys. Rev. Lett. **107**, 206805 (2011).
[17]P. C. Kelires, Europhys. Lett. **14**, 43 (1991); Phys. Rev. Lett. **73**, 2460 (1994); Appl. Surf. Sci. **102**, 12 (1996).
[18]J. Tersoff, Phys. Rev. B **39**, 5566 (1989).
[19]S. Munetoh, T. Motooka, K. Moriguchi, and A. Shintani, Comp. Mater. Sci. **39**, 334 (2007).
[20]T. Demuth, Y. Jeanvoine, J. Hafner, and J. G. Angyan, J. Phys. Condens. Matter **11**, 3833 (1999).
[21]J. Chen, G. Zhang, and B. Li, J. Appl. Phys. **112**, 064319 (2012).
[22]S. Godefroo, M. Hayne, M. Jivanescu, A. Stesmans, M. Zacharias, O. Lebedev, G. van Tendeloo, and V. Moshchalkov, Nat. Nanotechnol. **3**, 174 (2008).
[23]The optical response and energetics of defects will be presented elsewhere.
[24]R. Brückner, J. Non-Cryst. Solids **5**, 123 (1970).
[25]Y. Inamura, M. Arai, M. Nakamura, T. Otomo, N. Kitamura, S. Bennington, A. Hannon, and U. Buckenau, J. Non-Cryst. Solids **293**, 389 (2001).
[26]P. C. Kelires and J. Tersoff, Phys. Rev. Lett. **63**, 1164 (1989).
[27]P. Sonnet and P. C. Kelires, Phys. Rev. B **66**, 205307 (2002); Appl. Phys. Lett. **85**, 203 (2004).
[28]G. Vantarakis, I. N. Remediakis, and P. C. Kelires, Phys. Rev. Lett. **108**, 176102 (2012).
[29]K. Kusová, L. Ondič, E. Klimeššová, K. Herynková, I. Pelant, S. Danisš, J. Valenta, M. Gallart, M. Ziegler, B. Hönerlage, and P. Gilliot, Appl. Phys. Lett. **101**, 143101 (2012).
[30]M. V. Wolkin, J. Jorne, P. M. Fauchet, G. Allan, and C. Delerue, Phys. Rev. Lett. **82**, 197 (1999).
[31]A. Puzder, A. J. Williamson, J. C. Grossman, and G. Galli, Phys. Rev. Lett. **88**, 097401 (2002).
[32]I. Vasiliev, J. R. Chelikowsky, and R. M. Martin, Phys. Rev. B **65**, 121302 (2002).
[33]E. Luppi, F. Iori, R. Magri, O. Pulci, S. Ossicini, E. Degoli, and V. Olevano, Phys. Rev. B **75**, 033303 (2007).
[34]B. Lee, D. Hiller, J.-W. Luo, O. Semonin, M. Beard, M. Zacharias, and P. Stradins, Adv. Funct. Mater. **22**, 3223 (2012).
[35]T. J. Pennycook, G. Hadjisavvas, J. C. Idrobo, P. C. Kelires, and S. T. Pantelides, Phys. Rev. B **82**, 125310 (2010).